Start Small: A Model for Tissue-wide Planar Cell Polarity without Morphogens

Abhisha Thayambath[1,2] and Julio M Belmonte[1,2]

[1]Department of Physics, North Carolina State University, Raleigh, North Carolina, USA
[2] Quantitative and Computational Developmental Biology Cluster, North Carolina State University, Raleigh, North Carolina, USA

Corresponding author: jbelmon2@ncsu.edu

Abstract

Planar cell polarity (PCP) is an important patterning mechanism in both vertebrates and invertebrates by which cells coherently polarize along the apical surface of the epithelium. This patterning mechanism acts upstream of many developmental processes, such as oriented growth, division, cell movements and orientation of body hairs. While various models have been proposed to explain PCP patterning, all rely on persistent global cues/gradients to obtain global orientation of large tissues. However, recent experimental work has shown that this process can happen independently of such global cues, challenging the current paradigm. In this work, we developed a new model for PCP using the Cellular Potts modelling framework to investigate the conditions under which global tissue orientation can be achieved without a tissue spanning morphogen. We found that a combination of a local boundary signal, a small initial tissue size and uniform proliferation can effectively establish long-range polarity without the need for global cues.

Introduction

Cell polarity is the intrinsic asymmetry in the shape, structure, or spatial organization of cellular components that enables cell and tissues to perform specialized functions. The initial phase in the development of multicellular organisms involves the organization of cells into an epithelial sheet, marking the first step in the establishment of tissue polarity. Cells polarize along the apical-basal axis with the apical membrane facing the lumen and the baso-lateral membrane connecting each cell to the neighbouring cells and to the extra-cellular matrix. This polarized epithelial sheet undergoes dramatic remodelling that generates the germ layers which later gives rise to all tissues and organs in the body. In addition to apical-basal polarity, epithelial sheets also exhibit polarity in an orthogonal direction, within the plane of the apical surface, called **Planar Cell Polarity (PCP)**. PCP is an important patterning mechanism across metazoan epithelial tissues that is used for the generation of body hairs (sensory hairs in mammals [1][2], wing hair in *Drosophila* [3] etc.) and the orientation of tissue processes such as convergent-extension that generates the head-to-tail body axis in vertebrates [4], and neural tube closure [5].

The mechanisms underlying planar cell polarity have been extensively studied in *Drosophila* where PCP controls the orientation of hairs on the wing and abdomen and the organization of ommatidia in the eye [6]. Two major pathways establish PCP in *Drosophila* wing- the **core PCP pathway** and the **Fat–Dachsous pathway**. Both pathways rely on the asymmetric localization of their associated proteins on the opposing sides of each cell. This asymmetric localization is guided in part by direct communication between neighbouring cells which determines local alignment, and by a putative global cue which determines the global direction of tissue polarization.

The core pathway is composed of the cytoplasmic proteins Dishevelled(Dsh), Diego(Dg) and Prickle(Pk), transmembrane proteins Frizzled(Fz) and Van Gogh/Strabismus(Van/Stbm) and an atypical cadherin Flamingo(Fmi). Fmi is found on both opposing ends of each cell, and facilitates homophilic cell adhesion between adjacent cells [7] [8]. The communication between neighboring cells occurs through the

interaction of Fz–Fmi in one cell with Vang–Fmi in the adjacent cell. Inside a cell, Dsh binds with Fz [9], whereas Pk interacts with Van [10]. Pk also binds to Dsh preventing it from localizing to the proximal side [11] by destablizing Fz binding [12]. Diego competes with Pk for Dsh binding favouring Dsh accumulation on the distal side and thereby enhancing Fz localization at the distal membrane [13]. As a result of this competitive inhibition, the complexes Van-Pk and Fz-Dsh-Dg localize to the opposing ends of each cell, forming the cells' proximal and distal domains, respectively [14][15][16] (see [17] and [18] for review).

The Ft-Ds pathway is composed of the protocadherins Ft and Ds which form heterophilic complexes between cells [19]. This is regulated by the transmembrane kinase Four-Jointed (Fj). In the developing wing, the asymmetric localization of Ft to the proximal side and Ds to the distal sides of the cells is driven by the complementary gradients of Ds and Fj [20][21]. It is still unclear whether the Ft-Ds pathway operates independently or together with the core pathway to coordinate polarity across the tissue [22][23].

Experiments and mathematical models suggest that the spatial segregation of polarity complexes inside each cell and their preferential affinity between neighbouring cells is effective in coordinating polarity across small groups of cells. An initial uniform distribution of these core proteins spatially segregates over time, resulting in a polarized distribution (Figure 1A); however, what leads to the spontaneous breaking of this initial symmetry is still unknown. While the reinforcement of the initial asymmetry by feedback interactions is sufficient for the local coordination of cell polarities, the identity of the biasing cue that could determine the global alignment direction and ensure large-scale coordination remains poorly understood. It has been hypothesized that the global alignment of core PCP proteins may arise from a spatial gradient of a biasing cue acting across the entire tissue. Lawrence et al. have shown that if the spatial gradient of a secreted molecule acts as the global cue, then it is not part of the DPP, Notch, EGF, or FGF signalling pathways [24]. The Ft-Ds-Fj system is thought to be a potential candidate that could act as an upstream global cue for the core proteins, given that Ds and Fj are expressed in complementary gradients in opposing directions. However, even in conditions of uniform expression of these components, polarity can still be effectively established, suggesting that the gradients of Ft-Ds-Fj are not strictly necessary [25] (see [26] for a comprehensive review).

Wnt ligands, which bind to Fz receptors, are expressed as gradients in the developing Drosophila wing [27][28][29]. Together, they recruit and activate Dsh, which is also a highly conserved component of the Wnt signalling pathway, which in turn propagates the signal internally to the cell [30]. Since Fz and Dsh belong to the core pathway, Wnt was long considered to be the global cue that sets the global alignment and long-range orientation of the PCP in *Drosophila* wing and other PCP systems. Although some studies have suggested the role of Wnt ligands (Wg and Wnt4) in global PCP establishment [31], two independent recent studies show that Wnt ligands are not required to align core PCP in *Drosophila* [32] [33]. Ewen-Campen et al. conducted loss of function studies targeting different combinations of Wg and other Wnt genes (wnt2, wnt4, wnt5, wnt6, wntD, wnt10) in *Drosophila* wing and notum and found that loss of individual or combinations of Wnt ligands that they examined do not disrupt PCP alignment [32]. In another study published in the same year, Yu et al. knocked out the diffusible Wnts DWnt2, Dwnt4, DWnt6, and DWnt10 and found no disruptions in wing hair orientation [33]. Together, these results show that Wnt ligands are not required for global PCP establishment, and other mechanisms must be responsible for the long-range orientation of PCP.

There are various models that explain the mechanisms behind planar cell polarity- ranging from explicit molecular signalling models to phenomenological/reduced models. The *explicit signalling models* consider the detailed interactions between the proteins in core and Ft-Ds pathways. For instance, both [34] and [35] describe cell polarity based on the asymmetric distribution of intercellular protein complexes with cells and their associated PCP components modelled by reaction-diffusion equations. Both models use a global cue (which could arise from a directional signal within each cell or from a tissue wide ligand gradient) to introduce a small bias in each cell which are enhanced by local feedback interactions between the core proteins. Fisher and colleagues [36] have shown that both these models require a persistent global cue to generate a robust polarity that is insensitive to noise.

The *phenomenological models* simplify the PCP mechanism by reducing the complexity of the spatial protein interactions in order to extract the fundamental interactions leading to planar polarization. Burak et al. [37] proposed a semi-phenomenological model that incorporates the mutual exclusion of Fz and Vang in individual cells along with the intercellular interactions. In this model, a weak global orienting signal, present during early development, is sufficient to establish long-range polarity. Wang et al. [38] used a cellular automata model to show how cells adjust their polarity with respect to the average polarity of their neighbours. They found that a strong global aligning cue generates faster

alignment of polarity. All these models used cells with a fixed shape in a fixed lattice. The work by Zhu and colleagues [39] was the first to use cells with varying shapes and dynamic neighbourhoods to study the effect of directional cue and hexagonal packing on the propagation of PCP. They found that the directional cue plays a critical role in establishing normal PCP, whereas hexagonal packing has a minimal effect on patterning. Schamberg et al. [40] developed a feedback and diffusion-based model that generates polarization in a row of cells, either through a weak initial global polarization across all cells or via a travelling wave originating from a single cell or boundary. Abley et al. [41] show that individual cells can polarize through random fluctuations and spread polarity via cell-cell coupling and boundary organizers. This model also used gradients to improve the tissue-level polarity. Hazelwood and Hancock [42] developed a functional model using global cues to study the molecular functions of core proteins Pk and Dsh. Fisher et al. [43] explored how intercellular protein complexes interpret tissue-wide gradients when establishing polarity. More recently, Singh and colleagues [44] developed a minimal model to investigate the emergence and robustness of planar cell polarity (PCP) through intercellular interactions and tissue-level gradients. Their model focusing on Ft-Ds heterodimer formation shows that while PCP can emerge without a global gradient, a global gradient is necessary to ensure robustness against noise and stabilize polarity patterns.

All these models, explicit and phenomenological, used a global cue - whether as a persistent directional signal within each cell, a tissue-wide ligand gradient, or a weak orienting signal - to establish and maintain the polarity across the tissue. However, given the recent experimental results by [32] [33] which found no evidence for the necessity of a Wnt gradient for the establishment and maintenance of PCP in the *Drosophila* wing (the primary model system for PCP), the question arises as whether there are morphogen-independent mechanisms that can explain robust establishment of long-range tissue orientation.

An alternative mechanism for PCP alignment in large tissues relies on cell shape changes. Aigouy et al. [45] proposed a vertex model where anisotropic tensions orient cell elongations, divisions, and rearrangements, leading to a global realignment of PCP along the direction of the applied tension. In 2012, Salbreux et al. [46] developed a model of zebrafish retina development where tissue-scale mechanical stresses induce cell elongation and promote PCP orientation along the elongated axis. Sugimura et al. [47] proposed a reduced model suggesting that anisotropy from cell elongation along with asymmetric cell-cell coupling along a particular axis can act as a global cue for polarity alignment. However, all these models are based either on a pre-established PCP order from which the applied tension realigns the orientation [45] [47] or on a specific sequence of PCP activation of cell rows that facilitates global tissue alignment [46].

To address the question of how a tissue achieves large-scale PCP alignment without morphogens, we develop a phenomenological model for PCP based on the Cellular Potts (Glazier-Graner-Hogeweg) modelling framework in which we represent the asymmetrically distributed PCP proteins as distinct compartments inside cells [48] [49]. We implement the mutual exclusion of these compartments inside cells and intercellular signalling using the differential adhesion properties of these compartments. As discussed by Lavalou and Lecuit, adhesion motifs in the transmembrane PCP proteins play an essential role in forming the inter-cellular protein complexes in such a way that when one protein is expressed at a given cell boundary, its corresponding counterpart is also recruited to the interfacial boundary of the adjacent cell [18]. In our model, the compartments representing the proximal and distal PCP proteins at adjacent cell boundaries interact with a higher adhesion strength, leading to their preferential binding. Within each cell, these compartments exhibit low affinity for each other, leading to their spatial segregation. Through these interactions alone, we show that cells can locally align their polarity in the absence of a directional signal; while a boundary-orienting signal can polarize cells closer to the boundary. However this mechanism alone is not sufficient to establish a long-range direction of orientation and swirling patterns arise as we increase tissue size. To explore how we can establish and maintain global alignment along a particular direction across large numbers of cells, we examine and test a mechanism first suggested by Sagner et al. [50], where a small-scale alignment generated by the boundary signal can propagate as the tissue grows. Our results show that uniform cell proliferation coupled with a boundary signal is a robust mechanism for large-scale polarity establishment in the absence of a tissue-wide morphogen gradient. We also reproduce the domineering non-autonomous behaviour of the mutant PCP clones [34] and observe swirling patterns in the absence of a directional cue for large tissues.

Model Overview

We developed our model within the Cellular Potts Modelling framework, using the CompuCell3D (CC3D) simulation software [51]. This modelling framework represents cells as extended objects formed by a collection of lattice sites on a square or hexagonal grid in 2D or 3D. Each cell consists of either a single domain of lattice sites (defined by a domain ID and a domain type) or multiple domains representing specific sub-cellular compartments (e.g., nucleus and cytoplasm) or abstract regions inside cells (e.g., apical and basal regions). In our model, we represent each biological cell as a 2D object subdivided into four sub-cellular compartments/domains: (i) proximal, (ii) distal, (iii) lateral, and (iv) cytoplasm. Together they represent the spatial heterogeneity in the distribution of various PCP proteins as well as the cytosolic constituents of the cell as viewed from their apical side (Figure 1B'). Since each biological cell in our model is made up of the four domains, we assign a cluster ID to each domain to clearly indicate its association with a specific biological cell (Figure 1B). Proximal and distal domains represent the proteins that localize to the proximal (Fz, Dsh, Dgo) and distal (Van/Stbm, Pk) regions of the cells whereas the lateral domain represents the regions of the cell membrane not populated by the core PCP proteins.

An effective energy equation H_{total} defines the properties of each of these domains, such as size, aspect ratios, adhesion preferences, and interactions with other domains (Eq. 1). Each of these properties is governed by an individual term in the overall effective energy equation: a volume constraint H_V helps to maintain the size and compressibility of cell domains and a contact/adhesion energy (H_C) specifies the relative strength of contact/adhesion between domains from the same and/or different cells.

$$H_{total} = H_V + H_C \tag{1}$$

The system evolves by minimizing the effective energy H_{total} by a series of random lattice-site copy attempts where we randomly select a lattice site i and a neighbouring lattice site j within the 3rd neighbour order of i. If the two lattice sites belong to different cells or cell domains, we evaluate the difference in energy (ΔH) if the ID of site i is copied over site j. Lattice site copy attempts that decrease the effective energy of the system is accepted, whereas those that increase the effective energy of the system are accepted with a probability:

$$P = \exp\left(-\frac{\Delta H}{T}\right) \tag{2}$$

where T is a parameter that specifies the level of membrane fluctuations in the system. The unit of time of the simulations is the Monte-Carlo step (MCS), defined as N lattice-site copy attempts, where N is the number of lattice sites in the grid.

The volume constraint (H_V) penalizes the deviations of the cell domain's volume (V) - defined as the number of lattice sites occupied by the cell domain - from its target volume (V_t):

$$H_V = \lambda_V (V - V_t)^2 \tag{3}$$

where λ_V represents the strength of the volume constraint and can be interpreted as the inverse compressibility of the cell domain.

The contact energy (H_C) is modelled as:

$$H_C = \sum_i \sum_{j \neq i} J(\sigma_i, \sigma_j) \tag{4}$$

where the second sum is over the 4th order neighbours of site i; σ_i and σ_j are the types of cell compartments occupying sites i and j, respectively; and J is a matrix containing the contact/adhesion energy between compartment types belonging to the same cell and different cells.

The value of the J matrix is different depending on whether the domains belong to the same cell (same cluster ID) or to different cells (different cluster IDs). When belonging to the same cell, all contact energies of pairwise combinations of domains are set at low values, while those between the proximal and distal domains are set at high values to facilitate the sorting of the two domains inside the cells (Table 1). Even in the absence of a neighbour or an interacting environment, the proximal and distal domains segregate to opposing ends inside a cell in relatively faster time scales (Figure S1 A), and hence individual cells are capable of establishing PCP asymmetry autonomously in our model. This is consistent with the findings of [52] where individual cells lacking the core protein Fmi - and thus are unable to communicate with neighbouring cells - still generate PCP asymmetry.

Table 1: *Internal* contact energies between PCP domains

Cell Type	Proximal	Distal	Lateral	Cyto
Proximal	-	30	1	1
Distal	-	-	1	1
Lateral	-	-	-	1
Cyto	-	-	-	-

When belonging to different cells, all contact energies of pair-wise combinations of domains are set to higher values. We define the external adhesion energies in such a way that proximal and distal domains of neighbouring cells would preferentially bind together to incorporate the observed inter-cellular coupling (Table 2). We determined the exact values for each contact energy term by extensive parameter scans aimed at optimizing polarization for small systems.

Table 2: *External* contact energies between PCP domains

Cell Type	Proximal	Distal	Lateral	Cyto	Medium
Proximal	12	7	12	30	10
Distal	-	12	12	30	10
Lateral	-	-	14	30	14
Cyto	-	-	-	50	30
Medium					0

We also use a temporary cell type, called **seed** cells, to initialize the simulations by randomly placing them as seeds within the lattice and allowing them to grow into arbitrary shapes until they reach the target volume of a biological cell. During this growth phase, cells remodel their shapes and rearrange their neighbours to achieve efficient packing within the lattice. This mechanism is consistent with the observation that epithelial cells are usually irregularly packed, as in the case of the *Drosophila* wing during larval and pre-pupal stages, where repacking into a hexagonal array occurs after polarization and PCP proteins are thought to play a role in this process [53]. Once the cells reach the size of biological cells and relax their boundaries, we establish PCP domains within each cell by assigning them random spatial distributions within each cell (50% of cell volume is composed of cytoplasmic domains, 15% is composed of proximal domains and distal domains each and the remaining 20% is composed of the lateral domains). This random assignment is done to avoid imposing any pre-pattern on the tissue. The total volume of each domain inside each cell remains conserved throughout the simulation, unless there is cell growth. Starting from a homogeneous distribution, differential adhesion within individual cells and between neighbouring cells leads to the spatial segregation of PCP proteins inside each cell (Figure 1B', C). We observe that this intercellular coupling through stronger adhesion between prox-dist domains across cell boundaries is sufficient for local coordination of polarity in the absence of a directional cue. The proximal and distal domains segregate to opposite ends of each cell, with lateral compartment symmetrically localizing between them. This rearrangement occurs naturally, as the adhesion energies are set to prevent the direct contact between proximal and distal domains with the lateral compartment acting as a buffer between them. The system globally aligns along a random direction on a relatively short timescale of $30,000$ MCS for a system of 4×4 cells (Figure S1B, first panel).

In order to quantify the degree of tissue polarization, we adapted the order parameter used by the flocking model community to describe the collective movement of self-propelled particles [54][55]. Here, we describe every cell in the lattice using a polarity vector ($\vec{\nu}(\sigma)$) defined as the normalized distance between the center of mass of **proximal** and **distal** domains:

$$\vec{\nu}(\sigma) = \frac{\vec{r}(\sigma_{prox}) - \vec{r}(\sigma_{dist})}{|\vec{r}(\sigma_{prox}) - \vec{r}(\sigma_{dist})|} \tag{5}$$

where $\vec{r}(\sigma_{\text{prox}})$ and $\vec{r}(\sigma_{\text{dist}})$ are the positions of the center of mass of the **proximal** and **distal** domains of cell σ, respectively. From this vector, we define the scalar order parameter ϕ that describes the degree of global tissue polarization as

$$\phi = \frac{1}{N} \sum_{\theta} |\vec{\nu}(\sigma)| \tag{6}$$

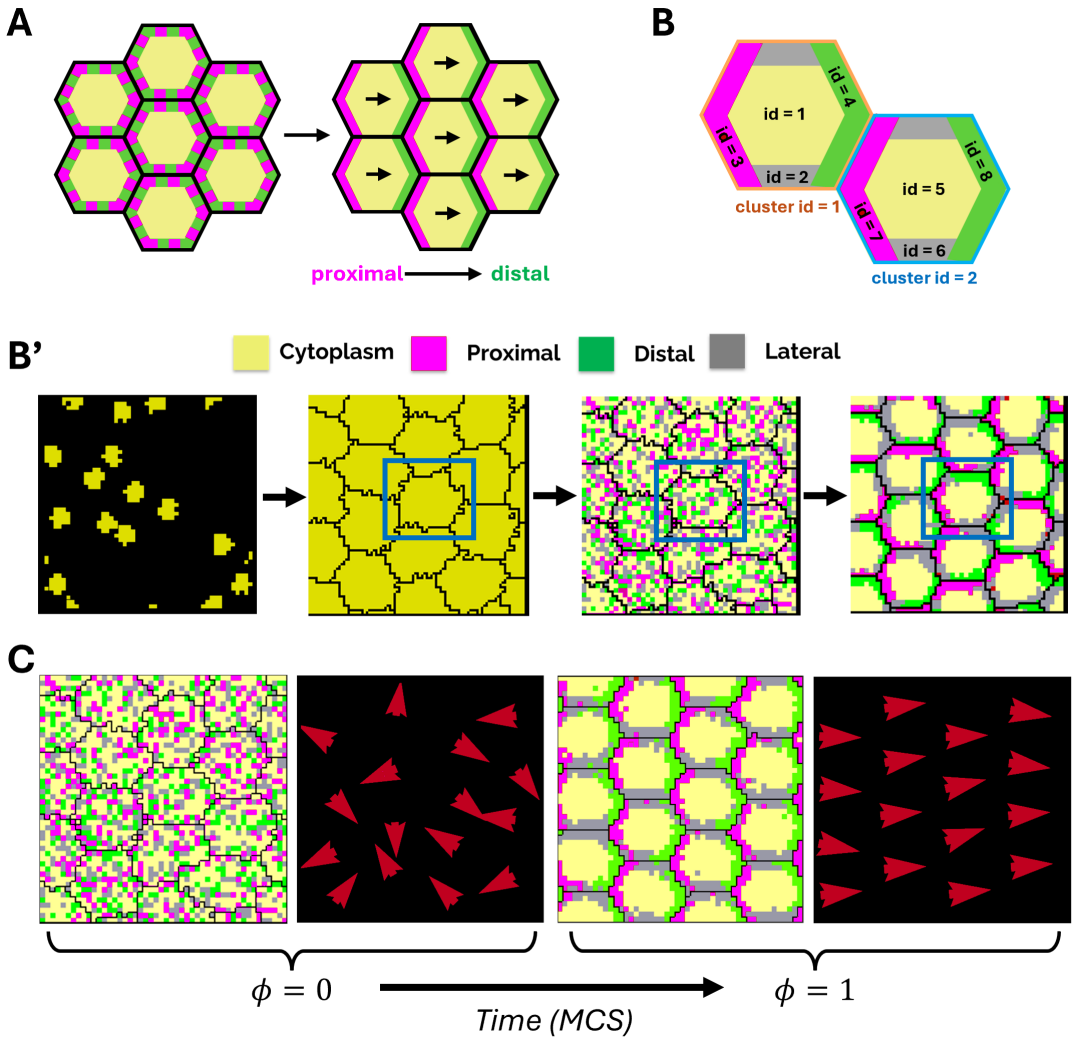

Figure 1: **Sub-cellular Potts Model for Planar Cell Polarity: (A)** Schematic of an epithelial cell arrangement with PCP protein distributions. Initially, the PCP proteins are uniformly distributed within each cell. Over time, Fz, Dsh, and Dgo (magenta) localize to the proximal/anterior edge, while Vang and Pk (green) segregate to the distal/posterior side. **(B)** Schematic of two epithelial cells with cluster ids 1 (orange) and 2 (blue) respectively, along with the respective domain ids. The cluster id indicates the association of each domain with a specific biological cell. **(B')** Model Overview: Each epithelial cell is subdivided into four compartments—proximal, distal, lateral, and cytoplasm. **Seed** cells are placed randomly within the lattice, which grow into arbitrary shapes to achieve the desired cell size and rearrange their neighbours to efficiently pack in the lattice. PCP domains are introduced with random initial distributions. The proximal and distal domains spatially segregate into opposing ends of each cell over time. **(C)** The vector field representation of PCP orientations shows the transition from a homogeneous distribution ($\phi = 0$) of global polarization to complete alignment ($\phi = 1$). (Panel A adapted from [17])

where N is the total number of cells in the lattice and $\phi \in [0, 1]$, where 0 means no alignment, and 1 means perfect alignment of PCP vectors (Figure 1C).

Results

Based on the modelling framework described in the previous section, we begin by studying the behaviour of the model under various scenarios and check if we can reproduce the previously known experimental results. We first examine the time evolution of the degree of global polarization across different boundary conditions. Then, we try to reproduce the cell non-autonomous effects in polarity alignment observed in *Vang* and *Fz* loss of function mutants. After this, we study the impact of increasing system size under different boundary conditions and investigate the mechanisms by which cells can establish long-range polarity. All results presented are averages over 100 independent simulations.

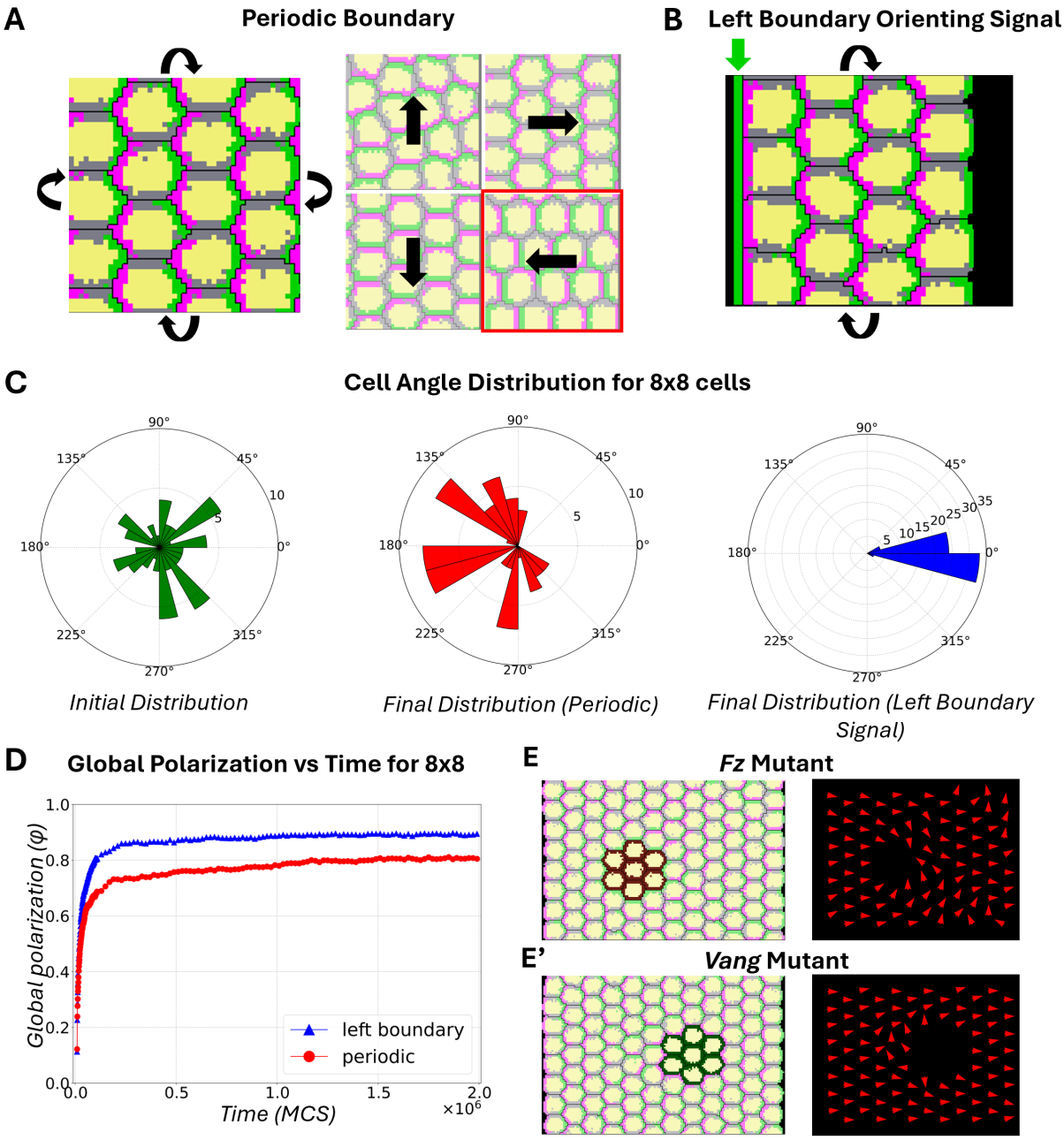

Figure 2: **Time Evolution of Global Polarization under different Boundary Conditions and Domineering Non-autonomy: (A)** Polarization outcomes under periodic boundary conditions applied along both the x and y directions. The system exhibits four distinct final states, with the mean tissue polarization vector aligning along one of the four directions: right, left, up, or down. **(B)** Polarization under a directional cue applied at the left boundary, with periodic boundary conditions maintained along the y axis. This configuration introduces a bias to the right and sets a definitive proximal-distal axis to the right. **(C)** Distribution of cell polarization angles in a system comprising 8×8 cells. The first panel (green) shows the initial distribution of cell polarization vectors. The second panel (red) depicts the final distribution under periodic boundary conditions, where the mean polarization aligns along the left direction, corresponding to the red-box outcome in (A). The third panel (blue) shows the final distribution under the left-boundary orienting signal, with polarization vectors highly aligned along the proximal-to-distal axis. **(D)** Time evolution of the global polarization, quantified by the scalar order parameter ϕ, under periodic (red circles) and left-boundary (blue triangles) conditions. In the periodic case, ϕ remains consistently lower. The left-boundary signal not only orients the polarization but also enhances the global alignment, leading to higher ϕ values in a system of 8×8 cells. **(E)** Domineering non-autonomous behaviour of cells in loss-of-function mutants for *Fz*. In *Fz* loss-of-function mutants (dark red), polarity vectors distal to the patch point towards the mutant clone. **(E')** Domineering non-autonomous behaviour of cells in loss-of-function mutants for *Vang*. In *Vang* loss-of-function mutants (dark green), polarity vectors proximal to the patch point away from the mutant clone.

Time Evolution of Global Polarization under different Boundary Conditions

We first characterized our model by investigating how it behaves under different conditions. We examined the evolution of global polarization over time under different boundary conditions for a system of 8×8 cells (Figure 2A, 2B). After a transient period of tissue growth and packing of 10^4 MCS, we introduced the PCP domains into the system and studied the evolution of global polarization defined by the scalar order parameter ϕ. As time increases from 10^4 MCS, global polarization increases and then stabilizes after 5×10^5 MCS for both the boundary conditions. (Figure 2D).

To circumvent the effects that an external boundary might have in tissue orientation, we first simulated our model with periodic boundary conditions. Under these boundary conditions, each cell has a complete set of neighbours, so these simulations can be viewed as a way to mimick a continuous and unbounded tissue. These boundary conditions help eliminate the edge effects present in large biological tissues by treating the tissue as if it wraps around on itself. Starting from an initial state where cell polarization vectors are randomly oriented (Figure 1C, first panel and Figure 2C, first panel, green), the system self-organizes toward a globally aligned state based only on the differential adhesion preferences between the domains inside and between cells without any imposed external cues. Over time, the global polarization increases and stabilizes at approximately 80% (Figure 2D, red). The final tissue angles of polarization are predominantly distributed along four distinct directions —right, left, up, and down—corresponding to the symmetry axes of the lattice (Figure 2A, second panel). Figure 2C (second panel) illustrates one such outcome in a small 8×8 system, where the initially random orientations of cell polarity vectors evolves toward the left, representing one of the possible final states under periodic conditions.

We also investigated the effect of boundary-orienting signals on tissue polarization. We added a fixed column of **distal** domain type at the left boundary of the system (Figure 2B), which acts as a directional cue that biases the global alignment direction towards the right (Figure 2C third panel, blue). The open boundary on the front does not have a preference for proximal or distal domains. The addition of this boundary signal not only biases the global alignment direction but also enhances the global polarization compared to the periodic boundary configuration for nearly all time steps in the simulation (Figure 2D). The mean angle of polarization is predominantly directed along the proximal-distal direction (Figure 2C, third panel, blue). From these results, we conclude that the presence of the boundary signal in our model successfully biases the system to polarize along a preferred direction.

Loss of Function Mutants produce Domineering Non-autonomy

Clones of cells lacking *Fz* function disrupt polarity in the wild-type cells distal to the mutant clones, whereas clones lacking *Vang* function disrupt polarity in wild type cells on the proximal side of the mutant clone [34]. This is called domineering non-autonomy because the mutant cells affect the polarity of the neighbouring wild-type cells. To test this in our model, we introduced a patch of cells that exhibit a loss of function for *Vang* or *Fz* activity. For *Fz*-like loss of function clones, we created a patch of cells where distal domains are absent, and instead, proximal domains fully populate the cell membrane (Figure 2E, dark red). We found that the polarity vectors distal to the mutant patch reoriented facing the mutant clone (Figure 2E). A similar technique was used to create *Vang*-like mutants, where we removed the proximal domains from a selected patch of cells while retaining only the distal domains (Figure 2E', dark green). We found that the polarity vectors in wild-type cells proximal to the mutant patch pointed away from the clone (Figure 2E'). Hence, our model successfully reproduces the domineering non-autonomous effects of *Fz* and *Vang* mutants.

Effect of System Size on Global and Local Polarization

After establishing the basic characteristics of the model and verifying that it is able to reproduce key results from experimental observations and other published models, we now investigate the effect of system size on global and local polarization. We increased the number of cells across different lattice sizes and ran simulations for 10^6 Monte Carlo Steps (MCS) to allow sufficient time for the system to polarize. As in the previous section, we considered two boundary conditions: periodic boundaries and left boundary signal (Figure 2A, B). We found that as the number of cells increases, global polarization decreases in both configurations (Figure 3A). In the periodic boundary configuration with 30×30 cells, the distribution of the mean angle of tissue polarization is nearly uniform (Figure 3B, first panel). However, for the left boundary configuration with 30×30 cells (Figure 3B, second panel), the mean angle does not exhibit the strong preference along the proximal-distal axis observed in the 8×8 system

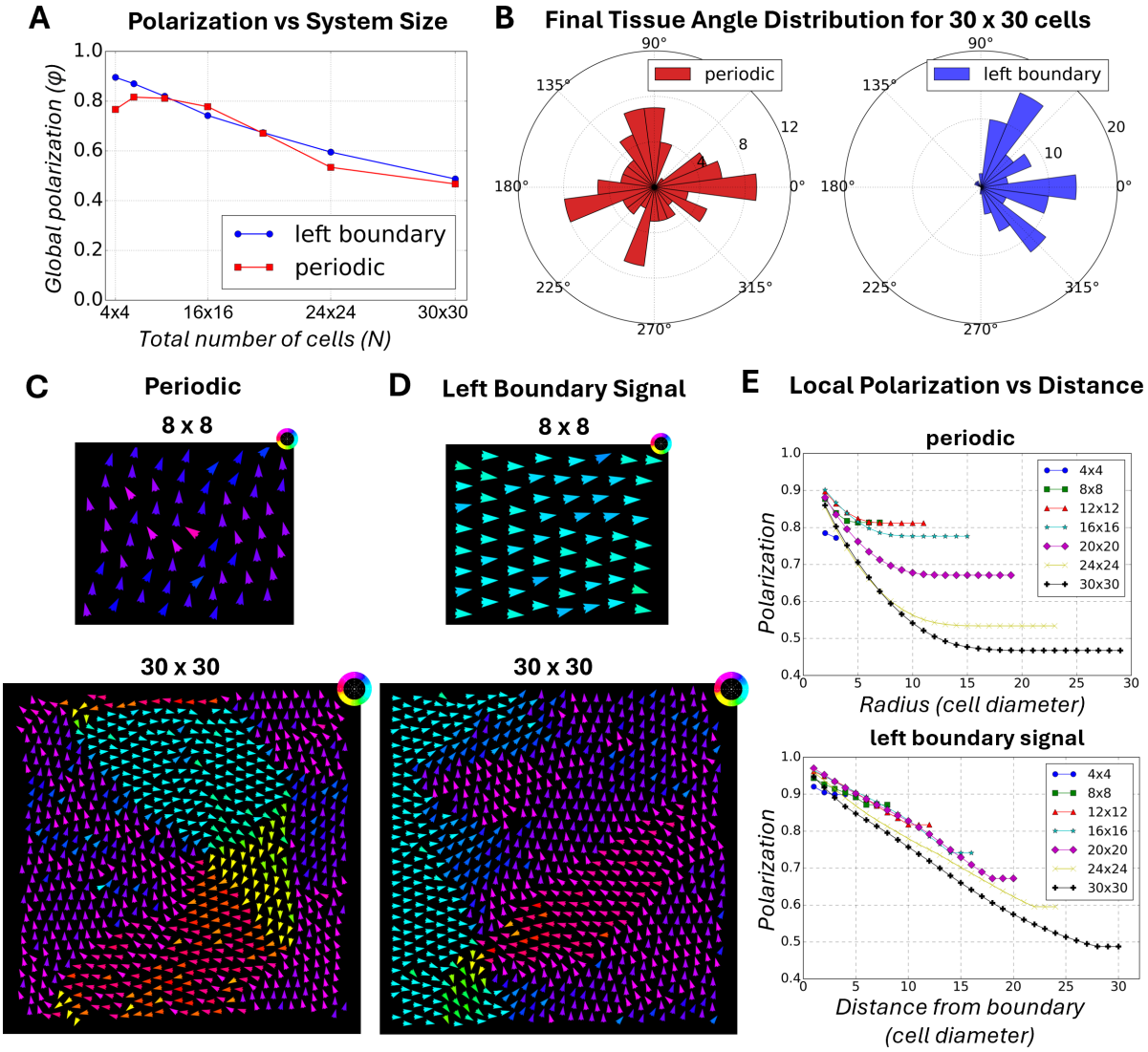

Figure 3: **Effect of System Size on Polarization for Periodic Boundary and Left Boundary Signal Configurations (A)** Final average global polarization (ϕ) for different system sizes under periodic and left boundary signal configurations (average over 100 simulations). As system size increases, global polarization decreases for both boundary conditions. **(B)** Final tissue angle distribution of polarization for the 30×30 system under periodic (red) and left boundary (blue) conditions. For periodic boundaries, the polarization angles become nearly uniform, while for the left boundary signal, the alignment direction is more dispersed around the proximal-distal axis. **(C)** Final cell polarity vectors for the 8×8 (top panel) and 30×30 (bottom panel) system with periodic boundary conditions. In the smaller 8×8 system, all cells align in a single direction (upward in this case). For the 30×30 system, local alignment occurs within small domains, and swirling patterns emerge. **(D)** Final cell polarity vectors for the 8×8 (top panel) and 30×30 (bottom panel) system with left boundary signal configuration. For the smaller 8×8 system, all cells align along proximal-distal direction. For the 30×30 system, alignment is maintained in the first few columns but dissipates as cells move farther from the boundary. **(E)** Local polarization as a function of radial distance for periodic boundary configuration (top panel) and as a function of distance from the boundary for left boundary signal configuration (bottom). Local polarization decreases sharply with distance in the periodic boundary case, whereas the decrease in polarization for the left boundary signal configuration is less steep.

(Figure 2C, third panel). Instead, the alignment direction is more dispersed around proximal-distal axis (Figure 3B, second panel). This suggests that the effect of the boundary orienting signal weakens with the distance from the boundary.

For the periodic boundary configuration, the representative simulation output for an 8×8 system shows that the final cell polarity vectors align along a specific direction (Figure 3C, top panel) while the 30×30 system shows that cells align within small local domains and swirling patterns emerge (Figure 3C, bottom panel). This clearly suggests that when system size increases, there is no long-range order across the entire system in the absence of a directional cue. For the configuration with the left boundary signal, 8×8 system shows cell polarity vectors aligned along proximal-distal axis (Figure 3D, top panel). However, when system size is increased to 30×30, although the first few columns of cells remain well aligned along proximal-distal axis, global alignment is lost as we move further away from the left boundary (Figure 3D, bottom panel).

We also examined how polarization changes as a function of distance. We defined the local polarization as the degree of tissue order parameter ϕ as a function of radial distance between cells (for periodic boundary configuration) or as a function of distance from the boundary signal. Local order is high (over 80%) over small distances (radius < 5 cell diameters), but decreases steeply as the radius (measured in units of cell diameters) increases for the periodic boundary configuration independently of tissue size (Figure 3E, top panel). This suggests that the distance over which the polarity alignment is maintained, the correlation length, is very small. In the left boundary signal configuration, cells close to the boundary are highly polalized with $\phi > 90\%$ for distancesup to 5 cell diameters. The degree of polarization still declines with distance from the boundary, but the decrease is less steep compared to the periodic case (Figure 3E, bottom panel). This indicates that the boundary signal helps maintain the cell polarity correlation higher and for longer distances as compared to periodic boundary configuration. However, it does not propagate tissue polarity effectively across large distances from the boundary. This reinforces the idea that additional mechanisms might be required for the coordination of polarity across a large tissue.

Cell Proliferation is Sufficient to Establish Long-range Polarity

Our findings from the previous section suggest that establishing polarity across a large tissue requires additional mechanisms. A key question is whether this can be achieved without a graded biasing signal acting across the entire tissue. We hypothesize that the cells may first establish polarity in a small domain with the help of a margin/boundary-oriented signal and then expand this domain while conserving alignment. To test this, we start with a small patch of tissue that is already polarized with the help of the left boundary-orienting signal. We then allow the cells to proliferate by gradually increasing their volume. We let these cells grow slowly while maintaining the relative proportions of the proximal, distal, lateral, and cytoplasmic domains so that the cells maintain their polarity during this process. When a cell exceeds twice its volume, it divides along its minor axis. Following division, daughter cells inherit equal fractions of the cell domains from the parent cell but lose internal polarity as we redistribute these domains uniformly within each daughter cell (Figure 4B). These cells re-polarize over time by spatially re-organizing their domains based on the polarity of the neighbouring cells. This mechanism is consistent with the findings from Devenport et al., where they describe how PCP components are equally inherited by daughter cells and how they re-establish their polarity in accordance with their neighbours in basal epidermal stem cells in mouse embryo [56].

We tested two different growth scenarios: growth at the distal end of the tissue (opposite to the boundary signal) and uniform tissue growth. We begin our simulations with a 10×4 system of cells that are already polarized. There is a periodic boundary condition along the vertical direction, a fixed boundary wall of **distal** domain type at the left side of the tissue, and an open space to the right that the tissue occupies as the cells grow and divide. The open boundary on the front has no preference between proximal and distal domains. We compare the results of the two scenarios to the polarization of tissues with fixed/pre-established sizes under the same boundary conditions that polarizes all at once. To allow for the comparison of growing tissues at different times, we varied the number of cell columns in the non-growing tissue.

As expected, for the simulations with fixed-sized tissues, the more cell columns we add, the smaller the global polarization, reaching $\phi = 0.3$ for the largest system size examined (Figure 4E, red line). The decrease in ϕ is steeper with increasing number of cells when compared to the previous case with square shaped tissues (Figure 2A first panel, 2B). In this case, each additional column of cells are farther away from the boundary signal, as the tissue has more cells along x-direction. This causes a steeper decline in

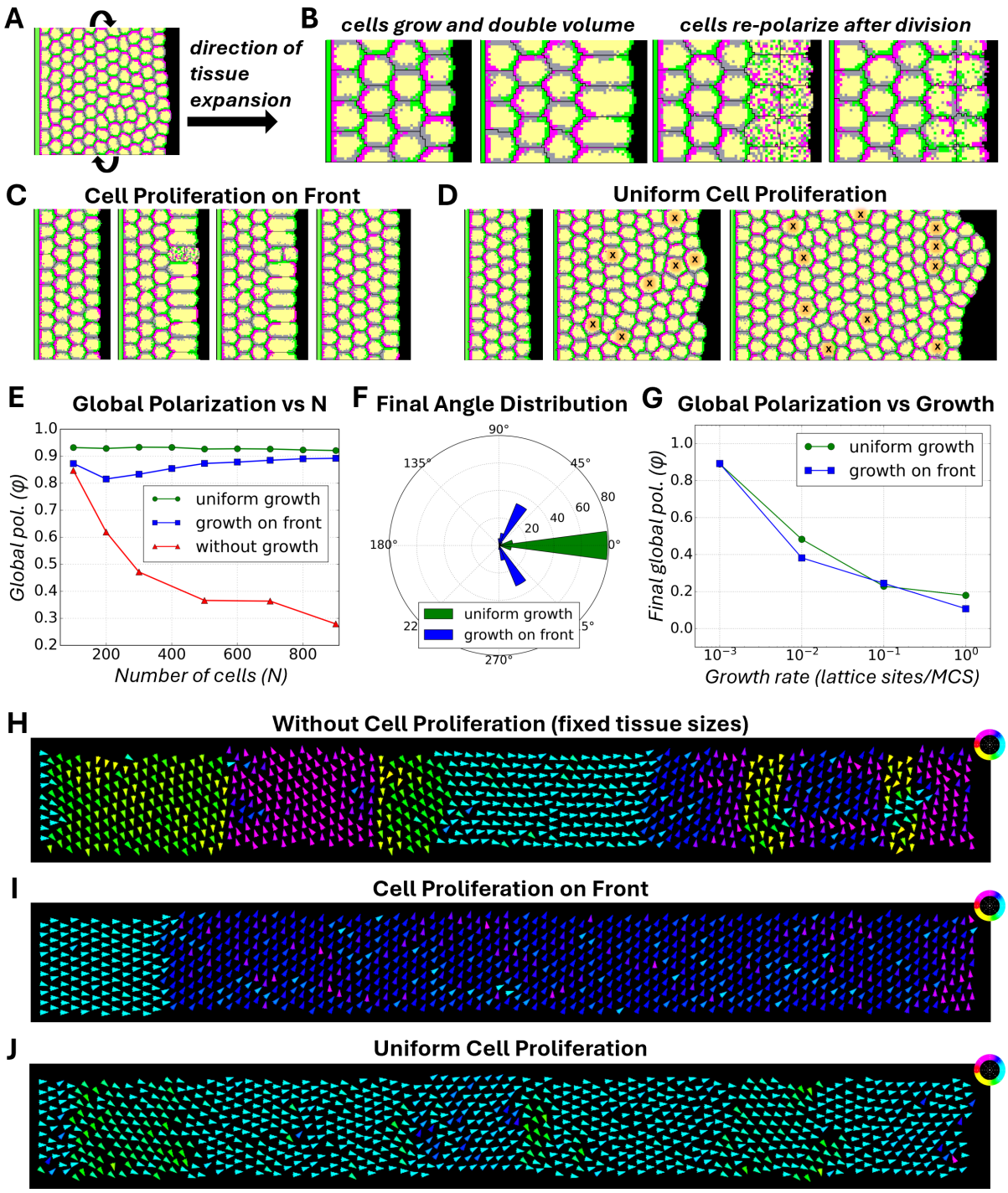

Figure 4: **Cell Proliferation-Based Mechanism for Maintaining Polarity.** **(A)** Schematic of the system used to study effect cell proliferation. 10 rows of cells are arranged in a box with periodic conditions along the vertical direction, a boundary signal on the left, and an open space on the right. **(B)** Cells grow to double their volume and then divide. After each division, daughter cells inherit the PCP domains equally, lose polarity, and redistribute these domains based on neighbouring cells' polarity. **(C)** Simulation showing cell growth and division at the distal/front boundary of a system. **(D)** Simulation showing uniform cell proliferation. Cells about to divide are inidicated by an 'X' mark. **(E)** Comparison of global polarization ϕ for systems with and without cell proliferation as a function of the number of cells. For fixed tissue sizes, global polarization decreases with system size (red). Systems with cell proliferation on front/distal boundary stabilize at a higher ϕ, approximately 0.89 (blue). Uniform cell proliferation further enhances global polarization at a higher value 0.92 (green). **(F)** Distribution of mean angle of polarization for systems with proliferating cells, showing a shift towards $\pm 60°$ for front/distal boundary proliferation and proximal-distal alignment for uniform cell proliferation. **(G)** Comparison of final global polarization when number of cells in the system is 900 for varying growth rates for front/distal proliferation (blue) and uniform cell proliferation (green). For uniform cell proliferation, the relaxation time between cell divisions is set to $10,000$ MCS. **(H)** Simulation output showing polarity vector alignment for the configuration without cell proliferation. Domains of local alignment can be observed. **(I)** Simulation output showing polarity vector alignment for the proliferation on front configuration. **(J)** Simulation output showing preference for alignment along the proximal-distal axis for the uniform cell proliferation configuration.

tissue polarization as a function of distance from boundary than the square tissue case, where cells are added on both directions (Figure 4E, S7).

Next, we tested whether pre-polarizing a small (10×4) tissue and allowing cells at the distal end to grow and divide would improve polarization. As the number of cells increases, we observe a decrease in global polarization ϕ until the system size reaches 200 cells (Figure 4E, S3). After this, ϕ gradually recovers and stabilizes at approximately 0.9 as system size reaches 900 cells (Figure 4E). This suggests that cell proliferation on the boundary may help maintain the initially established polarity. However, when we examine the mean angle distribution for these systems, we observe that the alignment is not strictly along the x-direction but instead shifts towards $\pm 60°$ (Figure 4F). Simulation snapshots confirms that after a few rows away from the left boundary, the polarity vectors tend to point either upward or downward, explaining the initial decrease observed in global polarization ϕ (Figure 4I, S2). This trend can be observed in the plot of local polarization as a function of distance from the boundary, where ϕ decreases with distance and stabilizes after approximately 20 columns of cells (Figure S7). The results presented are for growth rates of 0.001 lattice sites per MCS (or a 1.44×10^5 MCS volume doubling time). Results remain the same for slower growth rates, but polarization is gradually lost for faster growth rates, suggesting that cells need some time to adjust their polarity before the next round of division to maintain local tissue alignment (Figure S6). We found that slower growth rates help maintain the initially established polarity as the cells grow (Figure 4G, S6).

Instead of restricting cell growth to just the front boundary, we allow all cells to grow, but at randomly assigned times. The time at which each cell begins to grow is decided by selecting a random number between 0 and relaxation time t_{relax}. Once a cell reaches twice its initial volume, it divides. The newly divided cells would start to grow again only after a random time t_{random} (selected between 0 and t_{relax}) has passed. The growth rate is set to 0.001 lattice sites per MCS (or a 1.44×10^5 MCS volume doubling time). As a result, the time scale for polarity adjustment is much shorter than the growth and division time scale, giving the cell ample time to adjust its polarity between divisions. We find that the global polarization, ϕ, remains roughly constant at values greater than 0.9 as the number of cells in the system increases. Although there is a slight progressive drop in ϕ as the system size expands, ϕ stays above 0.9 up to a system size of 900 cells (Figure 4E). A similar trend is observed for the local order, which also remains above 0.9 (Figure S7). Unlike the previous growth scenario, the mean angle distribution plot shows that the system stays preferentially aligned along the proximal-distal axis. The simulation output also shows that the polarity vectors tend to point along the proximal-distal direction (Figure 4J). Thus, uniform cell proliferation appears to be an effective mechanism that robustly maintains the initially established polarity.

Discussion

Planar Cell Polarity is a key mechanism to establish the long range orientation of tissues along their apical surfaces. The establishment of a coherent proximal-distal axis is crucial for the proper function of many cellular and developmental processes downstream of PCP [57]. While the mechanisms of local planar cell polarity through direct cell-cell communication are well understood experimentally and computationally, the long-range order and direction of tissue orientation remains an open question. Multiple computational models suggest the need of some global cue for the establishment of tissue wide PCP alignment in the presence of noise. Yet, experimentally, the list of possible candidates for such a global cue continues to diminish. Early in 2000's, Peter Lawrence and colleagues showed that PCP is independent of the DPP, Notch, EGF, and FGF signalling pathways [24]. The Ds and Fj proteins, which are part of the Fat–Dachsous PCP pathway, are expressed in opposing gradients and could act together as the global cue. However, uniform expression of those components does not alter the long-range PCP alignment [25]. And more recent studies show that long-range PCP polarity in the *Drosophila* wing and notum can be established independent of Wnt gradients [32] [33]. All these negative results suggest that an alternative mechanism, independent of morphogen gradients, may be required to establish global PCP orientation.

PCP emerges in the *Drosophila* wing imaginal disc during larval stages and is aligned with respect to the signalling centers - Wingless (Wg) and Notch at the dorso-ventral boundary, Hedgehog (Hh) and Decapentaplegic (Dpp) at the anterior-posterior compartment boundary, and Dachsous (Ds) at the hinge fold [50]. These signalling centers may be acting as a boundary signals that orients the first row of cells and, subsequently, the other cells by the autonomous PCP alignment mechanism. Sanger et al. proposed that PCP may be established early in development, while the tissue is still small, with the guidance of local boundary signals, and long-range tissue orientation arises through subsequent cell proliferation [50].

To investigate how PCP behaves in large tissues in the presence of a local boundary signal, we created a stochastic phenomenological model of PCP dynamics that relies only on the contact affinities between cell compartments within and across cells. In our model, we systematically increased the number of cells in the system under different conditions. We found that a local boundary-orienting signal is not sufficient to establish long-range polarity. Although individual cells can asymmetrically segregate their proximal and distal domains in a short timescale (Figure S1 A) and reorient their polarity in accordance to their immediate neighbours, direct cell-cell communication is not sufficient to propagate directional information effectively and, as a result, cells do not align their polarity along the tissue proximal-distal axis. These results are in agreement with previous experimental and computational results. In their phenomenological model, Burak and Shraiman also found that a boundary-orienting signal cannot propagate polarity information across hundreds of cells within realistic timescales [37]. Cellular automata based models by Wang et al. show rows of cells that are already aligned near a boundary can influence the alignment of the rest of the cells in the lattice, however, is not efficient to coordinate polarity across the entire lattice [38].

Like all other models to date, we assume that the PCP proteins that make the distal and proximal domains have the ability to reorganize their spatial orientation using the local information provided by their immediate neighbours. Recently, Devenport and colleagues demonstrated experimentally that this assumption is true for mice epidermal cells [58]. By generating chimeric mouse embryos composed of cells expressing dual PCP reporters (*Fz6 3xGFP* and *tdTomato-Vangl2*) mixed with unlabelled cells that lack *Celsr1*, they show that homotypic *Celsr1* interactions between cells are required to sort *Vangl2* and *Fz6* to opposite sides of cell junction. Whether single cells have the ability to polarize cell autonomously, however, seems to be organism specific: in mice, cells are not able to polarize autonomously [58], while in *Drosophila* they can [52]. We chose our model parameters (see Table 2) to reflect the latter case; however, setting the internal contact energies to negative values to prevent cell-autonomous polarization still allows spontaneous tissue polarization, and the key results from our model remain qualitatively the same.

We then introduce cell proliferation in the presence of a boundary signal to investigate whether such a mechanism would maintain PCP orientation as the tissue grows. In our model for cell growth and division, we incorporated two important observations made in mammalian skin cells: that PCP components are inherited by daughter cells; and that cells lose their polarity information during division due to the temporary internalization of PCP proteins [56]. Therefore, cells in our model must reorient their proximal and distal compartments using only the local information from their immediate neighbours. Our results show that cell proliferation is sufficient to sustain and propagate the initially established polarity in an expanding tissue, as long as the timescale of cell growth is slow compared to the time scales associated with cell polarity rearrangement (Figure 4G). Aigouy et al. found that loss of Dachsous (Ds) disrupts PCP alignment at larval stages in *Drosophila* by interfering with cell divisions [45]. This implies that oriented cell divisions during larval stages may contribute to propagating polarity generated using the boundary signals. In our simulations, divisions planes along the minor axis of cell elongation produces higher PCP alignment than divisions at random orientation (Figure S4). When a cell undergoes division along its minor axis, the daughter cells share more surface area with surrounding neighbours than with each other. This increased contact with already polarized neighbours may enhance the integration of polarity cues. In contrast, division along the long axis results in daughter cells maintaining more surface contact with each other than with external neighbours, reducing their access to external polarity cues and leading to weaker polarization. Also, the daughter cells resulting from cell division along the long axis are initially elongated and their subsequent rounding up to minimize the surface energy further disrupts polarity rearrangement. Thus oriented cell growth and division can effectively establish a higher degree of polarization, confirming the role of oriented cell divisions in PCP alignment.

Our results also indicate a difference between allowing cells only at the front to proliferate and allowing all the cells in the tissue to divide at random times. We believe that the directional shift in polarity alignment observed for cell proliferation on the front scenario could be due to the lack of ability of the newly divided cells at the boundary to fully integrate polarity cues from all directions. However, when cell proliferation occurs uniformly throughout the tissue, each newly divided cell is surrounded by multiple neighbouring cells, enabling it to receive polarity information from all sides. As a result, uniform proliferation serves as a robust mechanism to establish long-range polarity that aligns with the direction specified by the boundary. Interestingly, in our simulations with front/distal cell proliferation, once the distal-most cells shift orientation to either ± 60 degrees, the new orientation remains coherent for the rest of the simulation. This suggests that when tissue growth is front-restricted, a near orthogonal PCP orientation with respect to the direction of tissue growth can be a robust mechanism to establish

long-range PCP orientation, albeit at a different orientation axis than the one set by the boundary signal.

This work presents the first description of planar cell polarity using the Cellular Potts Model, which offers a unique advantage by allowing for a detailed representation of cell behaviours in a dynamically evolving tissue environment. Most previous models have considered non-motile cells with fixed shapes [34][35][38][37], with some exceptions incorporating variations in cell shape [39] or allowing cells to divide, change shape, and rearrange their neighbours [45]. In our model, cells are highly dynamic — they can change shape, exchange neighbours, and actively pack themselves within the lattice through growth and rearrangement. Since PCP is also crucial for providing directional information and thereby guiding other developmental processes, our model based on Cellular Potts formalism provides a versatile framework for studying PCP-driven morphogenesis in other contexts for which Cellular Potts models have been used in the past, such as convergent-extension [59][60], limb-bud growth [61] and primitive streak formation [62].

Acknowledgements

We would like to thank Dr. Eric Brooks for his valuable feedback and comments on this work. We also thank Dr. François Graner and Dr. James Glazier for their feedback and assistance with the implementation of certain aspects of the model. We also thank Dr. Juan Manuel Gomez, Dr. Lutz Brusch, Dr. Benedikt Best and Pedro Cencil Dal Castel for their feedback and comments on this work. We acknowledge the computing resources provided by North Carolina State University High Performance Computing Services Core Facility (RRID:SCR_022168). This work was supported by the North Carolina State University.

Author contributions

JMB conceptualized the study. AT and JMB developed the computational model. AT conducted the investigation, formal analysis and visualization. AT and JMB wrote the manuscript.

Competing interests

The authors declare no conflicts of interest.

Materials and Methods

The model was developed using the CompuCell3D (CC3D) simulation software [51], with simulations executed on a computer cluster using a set of custom-developed Python scripts. The simulation code is publicly available at https://github.com/abhisha-ramesh/PCP_Subcellular_Potts_Model.

References

[1] Suzanne Eaton. "Planar polarization of Drosophila and vertebrate epithelia". en. In: *Current Opinion in Cell Biology* 9.6 (Dec. 1997), pp. 860–866. ISSN: 09550674. DOI: 10.1016/S0955-0674(97)80089-0.

[2] John B. Wallingford. "Planar Cell Polarity and the Developmental Control of Cell Behavior in Vertebrate Embryos". en. In: *Annual Review of Cell and Developmental Biology* 28.1 (Nov. 2012), pp. 627–653. ISSN: 1081-0706, 1530-8995. DOI: 10.1146/annurev-cellbio-092910-154208.

[3] D. Gubb and A. García-Bellido. "A genetic analysis of the determination of cuticular polarity during development in *Drosophila melanogaster*". en. In: *Development* 68.1 (Apr. 1982), pp. 37–57. ISSN: 0950-1991, 1477-9129. DOI: 10.1242/dev.68.1.37.

[4] Ray Keller. "Shaping the Vertebrate Body Plan by Polarized Embryonic Cell Movements". en. In: *Science* 298.5600 (Dec. 2002), pp. 1950–1954. ISSN: 0036-8075, 1095-9203. DOI: 10.1126/science.1079478.

[5] Zoha Kibar et al. "Ltap, a mammalian homolog of Drosophila Strabismus/Van Gogh, is altered in the mouse neural tube mutant Loop-tail". en. In: *Nature Genetics* 28.3 (July 2001), pp. 251–255. ISSN: 1546-1718. DOI: 10.1038/90081.

[6] Lisa V. Goodrich and David Strutt. "Principles of planar polarity in animal development". en. In: *Development* 138.10 (May 2011), pp. 1877–1892. ISSN: 1477-9129, 0950-1991. DOI: 10.1242/dev.054080.

[7] Tadao Usui et al. "Flamingo, a Seven-Pass Transmembrane Cadherin, Regulates Planar Cell Polarity under the Control of Frizzled". en. In: *Cell* 98.5 (Sept. 1999), pp. 585–595. ISSN: 00928674. DOI: 10.1016/S0092-8674(00)80046-X.

[8] Yuko Shimada et al. "Asymmetric colocalization of Flamingo, a seven-pass transmembrane cadherin, and Dishevelled in planar cell polarization". en. In: *Current Biology* 11.11 (June 2001), pp. 859–863. ISSN: 09609822. DOI: 10.1016/S0960-9822(01)00233-0.

[9] Hing-C. Wong et al. "Direct Binding of the PDZ Domain of Dishevelled to a Conserved Internal Sequence in the C-Terminal Region of Frizzled". In: *Molecular Cell* 12.5 (Nov. 2003), pp. 1251–1260. ISSN: 1097-2765. DOI: 10.1016/S1097-2765(03)00427-1.

[10] Rebecca Bastock, Helen Strutt, and David Strutt. "Strabismus is asymmetrically localised and binds to Prickle and Dishevelled during *Drosophila* planar polarity patterning". en. In: *Development* 130.13 (July 2003), pp. 3007–3014. ISSN: 1477-9129, 0950-1991. DOI: 10.1242/dev.00526.

[11] David R.P. Tree et al. "Prickle Mediates Feedback Amplification to Generate Asymmetric Planar Cell Polarity Signaling". en. In: *Cell* 109.3 (May 2002), pp. 371–381. ISSN: 00928674. DOI: 10.1016/S0092-8674(02)00715-8.

[12] Samantha J. Warrington et al. "A Dual Function for Prickle in Regulating Frizzled Stability during Feedback-Dependent Amplification of Planar Polarity". en. In: *Current Biology* 27.18 (Sept. 2017), 2784–2797.e3. ISSN: 09609822. DOI: 10.1016/j.cub.2017.08.016.

[13] Andreas Jenny et al. "Diego and Prickle regulate Frizzled planar cell polarity signalling by competing for Dishevelled binding". en. In: *Nature Cell Biology* 7.7 (July 2005), pp. 691–697. ISSN: 1476-4679. DOI: 10.1038/ncb1271.

[14] D. I. Strutt. "Asymmetric localization of frizzled and the establishment of cell polarity in the Drosophila wing". eng. In: *Molecular Cell* 7.2 (Feb. 2001), pp. 367–375. ISSN: 1097-2765. DOI: 10.1016/s1097-2765(01)00184-8.

[15] J. D. Axelrod. "Unipolar membrane association of Dishevelled mediates Frizzled planar cell polarity signaling". eng. In: *Genes & Development* 15.10 (May 2001), pp. 1182–1187. ISSN: 0890-9369. DOI: 10.1101/gad.890501.

[16] Gishnu Das et al. "Diego interacts with Prickle and Strabismus/Van Gogh to localize planar cell polarity complexes". en. In: *Development* 131.18 (Sept. 2004), pp. 4467–4476. ISSN: 1477-9129, 0950-1991. DOI: 10.1242/dev.01317.

[17] Danelle Devenport. "The cell biology of planar cell polarity". en. In: *Journal of Cell Biology* 207.2 (Oct. 2014), pp. 171–179. ISSN: 1540-8140, 0021-9525. DOI: 10.1083/jcb.201408039.

[18] Jules Lavalou and Thomas Lecuit. "In search of conserved principles of planar cell polarization". en. In: *Current Opinion in Genetics & Development* 72 (Feb. 2022), pp. 69–81. ISSN: 0959437X. DOI: 10.1016/j.gde.2021.11.001.

[19] Hitoshi Matakatsu and Seth S. Blair. "Separating the adhesive and signaling functions of the Fat and Dachsous protocadherins". en. In: *Development* 133.12 (June 2006), pp. 2315–2324. ISSN: 1477-9129, 0950-1991. DOI: 10.1242/dev.02401.

[20] Abhijit A. Ambegaonkar et al. "Propagation of Dachsous-Fat Planar Cell Polarity". en. In: *Current Biology* 22.14 (July 2012), pp. 1302–1308. ISSN: 09609822. DOI: 10.1016/j.cub.2012.05.049.

[21] Amy Brittle, Chloe Thomas, and David Strutt. "Planar Polarity Specification through Asymmetric Subcellular Localization of Fat and Dachsous". en. In: *Current Biology* 22.10 (May 2012), pp. 907–914. ISSN: 09609822. DOI: 10.1016/j.cub.2012.03.053.

[22] José Casal, Peter A. Lawrence, and Gary Struhl. "Two separate molecular systems, Dachsous/Fat and Starry night/Frizzled,act independently to confer planar cell polarity". en. In: *Development* 133.22 (Nov. 2006), pp. 4561–4572. ISSN: 1477-9129, 0950-1991. DOI: 10.1242/dev.02641.

[23] Helen Strutt and David Strutt. "How do the Fat–Dachsous and core planar polarity pathways act together and independently to coordinate polarized cell behaviours?" en. In: *Open Biology* 11.2 (Feb. 2021), p. 200356. ISSN: 2046-2441. DOI: 10.1098/rsob.200356.

[24] Peter A. Lawrence, José Casal, and Gary Struhl. "Towards a model of the organisation of planar polarity and pattern in the *Drosophila* abdomen". en. In: *Development* 129.11 (June 2002), pp. 2749–2760. ISSN: 1477-9129, 0950-1991. DOI: 10.1242/dev.129.11.2749.

[25] Hitoshi Matakatsu and Seth S. Blair. "Interactions between Fat and Dachsous and the regulation of planar cell polarity in the *Drosophila wing*". en. In: *Development* 131.15 (Aug. 2004), pp. 3785–3794. ISSN: 1477-9129, 0950-1991. DOI: 10.1242/dev.01254.

[26] Wen Yih Aw and Danelle Devenport. "Planar cell polarity: global inputs establishing cellular asymmetry". en. In: *Current Opinion in Cell Biology* 44 (Feb. 2017), pp. 110–116. ISSN: 09550674. DOI: 10.1016/j.ceb.2016.08.002.

[27] H.-Arno J. Müller, Reba Samanta, and Eric Wieschaus. "Wingless signaling in the *Drosophila* embryo: zygotic requirements and the role of the *frizzled* genes". en. In: *Development* 126.3 (Feb. 1999), pp. 577–586. ISSN: 0950-1991, 1477-9129. DOI: 10.1242/dev.126.3.577.

[28] Chiann-mun Chen and Gary Struhl. "Wingless transduction by the Frizzled and Frizzled2 proteins of *Drosophila*". en. In: *Development* 126.23 (Dec. 1999), pp. 5441–5452. ISSN: 0950-1991, 1477-9129. DOI: 10.1242/dev.126.23.5441.

[29] Purnima Bhanot et al. "Frizzled and DFrizzled-2 function as redundant receptors for Wingless during *Drosophila* embryonic development". en. In: *Development* 126.18 (Sept. 1999), pp. 4175–4186. ISSN: 0950-1991, 1477-9129. DOI: 10.1242/dev.126.18.4175.

[30] Monica Sharma et al. "Dishevelled: A masterful conductor of complex Wnt signals". en. In: *Cellular Signalling* 47 (July 2018), pp. 52–64. ISSN: 08986568. DOI: 10.1016/j.cellsig.2018.03.004.

[31] Jun Wu et al. "Wg and Wnt4 provide long-range directional input to planar cell polarity orientation in Drosophila". en. In: *Nature Cell Biology* 15.9 (Sept. 2013), pp. 1045–1055. ISSN: 1465-7392, 1476-4679. DOI: 10.1038/ncb2806.

[32] Ben Ewen-Campen et al. "No Evidence that Wnt Ligands Are Required for Planar Cell Polarity in Drosophila". en. In: *Cell Reports* 32.10 (Sept. 2020), p. 108121. ISSN: 22111247. DOI: 10.1016/j.celrep.2020.108121.

[33] Joyce J.S. Yu et al. "Frizzled-Dependent Planar Cell Polarity without Secreted Wnt Ligands". en. In: *Developmental Cell* 54.5 (Sept. 2020), 583–592.e5. ISSN: 15345807. DOI: 10.1016/j.devcel.2020.08.004.

[34] Keith Amonlirdviman et al. "Mathematical Modeling of Planar Cell Polarity to Understand Domineering Nonautonomy". en. In: *Science* 307.5708 (Jan. 2005), pp. 423–426. ISSN: 0036-8075, 1095-9203. DOI: 10.1126/science.1105471.

[35] Jean-François Le Garrec, Philippe Lopez, and Michel Kerszberg. "Establishment and maintenance of planar epithelial cell polarity by asymmetric cadherin bridges: A computer model". en. In: *Developmental Dynamics* 235.1 (Jan. 2006), pp. 235–246. ISSN: 1058-8388, 1097-0177. DOI: 10.1002/dvdy.20617.

[36] Sabine Fischer et al. "Is a persistent global bias necessary for the establishment of planar cell polarity?" eng. In: *PloS One* 8.4 (2013), e60064. ISSN: 1932-6203. DOI: 10.1371/journal.pone.0060064.

[37] Yoram Burak and Boris I. Shraiman. "Order and Stochastic Dynamics in Drosophila Planar Cell Polarity". en. In: *PLoS Computational Biology* 5.12 (Dec. 2009). Ed. by Anand R. Asthagiri, e1000628. ISSN: 1553-7358. DOI: 10.1371/journal.pcbi.1000628.

[38] Yanshu Wang, Tudor Badea, and Jeremy Nathans. "Order from disorder: Self-organization in mammalian hair patterning". en. In: *Proceedings of the National Academy of Sciences* 103.52 (Dec. 2006), pp. 19800–19805. ISSN: 0027-8424, 1091-6490. DOI: 10.1073/pnas.0609712104.

[39] Hao Zhu. "Is anisotropic propagation of polarized molecular distribution the common mechanism of swirling patterns of planar cell polarization?" en. In: *Journal of Theoretical Biology* 256.3 (Feb. 2009), pp. 315–325. ISSN: 00225193. DOI: 10.1016/j.jtbi.2008.08.029.

[40] S. Schamberg et al. "Modelling and Analysis of Planar Cell Polarity". en. In: *Bulletin of Mathematical Biology* 72.3 (Apr. 2010), pp. 645–680. ISSN: 0092-8240, 1522-9602. DOI: 10.1007/s11538-009-9464-0.

[41] Katie Abley et al. "An intracellular partitioning-based framework for tissue cell polarity in plants and animals". en. In: *Development* 140.10 (May 2013), pp. 2061–2074. ISSN: 1477-9129, 0950-1991. DOI: 10.1242/dev.062984.

[42] Lee D Hazelwood and John M Hancock. "Functional modelling of planar cell polarity: an approach for identifying molecular function". en. In: *BMC Developmental Biology* 13.1 (May 2013), p. 20. ISSN: 1471-213X. DOI: 10.1186/1471-213X-13-20.

[43] Katherine H. Fisher and David Strutt. "A theoretical framework for planar polarity establishment through interpretation of graded cues by molecular bridges". en. In: *Development* 146.3 (Feb. 2019), dev168955. ISSN: 1477-9129, 0950-1991. DOI: 10.1242/dev.168955.

[44] Divyoj Singh et al. "Emergence of planar cell polarity from the interplay of local interactions and global gradients". In: *eLife* 13 (Oct. 2024). Ed. by Karsten Kruse and Aleksandra M Walczak, e84053. ISSN: 2050-084X. DOI: 10.7554/eLife.84053.

[45] Benoît Aigouy et al. "Cell Flow Reorients the Axis of Planar Polarity in the Wing Epithelium of Drosophila". en. In: *Cell* 142.5 (Sept. 2010), pp. 773–786. ISSN: 00928674. DOI: 10.1016/j.cell.2010.07.042.

[46] Guillaume Salbreux et al. "Coupling Mechanical Deformations and Planar Cell Polarity to Create Regular Patterns in the Zebrafish Retina". en. In: *PLoS Computational Biology* 8.8 (Aug. 2012). Ed. by Stanislav Shvartsman, e1002618. ISSN: 1553-7358. DOI: 10.1371/journal.pcbi.1002618.

[47] Kaori Sugimura and Hiroshi Kori. "A reduced cell-based phase model for tissue polarity alignment through global anisotropic cues". en. In: *Scientific Reports* 7.1 (Dec. 2017), p. 17466. ISSN: 2045-2322. DOI: 10.1038/s41598-017-17611-8.

[48] François Graner and James A. Glazier. "Simulation of biological cell sorting using a two-dimensional extended Potts model". en. In: *Physical Review Letters* 69.13 (Sept. 1992), pp. 2013–2016. ISSN: 0031-9007. DOI: 10.1103/PhysRevLett.69.2013.

[49] J. A. Glazier and F. Graner. "Simulation of the differential adhesion driven rearrangement of biological cells". eng. In: *Physical Review. E, Statistical Physics, Plasmas, Fluids, and Related Interdisciplinary Topics* 47.3 (Mar. 1993), pp. 2128–2154. ISSN: 1063-651X. DOI: 10.1103/physreve.47.2128.

[50] Andreas Sagner et al. "Establishment of Global Patterns of Planar Polarity during Growth of the Drosophila Wing Epithelium". en. In: *Current Biology* 22.14 (July 2012), pp. 1296–1301. ISSN: 09609822. DOI: 10.1016/j.cub.2012.04.066.

[51] Maciej H. Swat et al. "Multi-Scale Modeling of Tissues Using CompuCell3D". en. In: *Methods in Cell Biology*. Vol. 110. Elsevier, 2012, pp. 325–366. ISBN: 9780123884039. DOI: 10.1016/B978-0-12-388403-9.00013-8.

[52] Alexis T Weiner et al. *Cell autonomous polarization by the planar cell polarity signaling pathway*. en. Sept. 2023. DOI: 10.1101/2023.09.26.559449.

[53] Anne-Kathrin Classen et al. "Hexagonal Packing of Drosophila Wing Epithelial Cells by the Planar Cell Polarity Pathway". en. In: *Developmental Cell* 9.6 (Dec. 2005), pp. 805–817. ISSN: 15345807. DOI: 10.1016/j.devcel.2005.10.016.

[54] Tamás Vicsek et al. "Novel Type of Phase Transition in a System of Self-Driven Particles". en. In: *Physical Review Letters* 75.6 (Aug. 1995), pp. 1226–1229. ISSN: 0031-9007, 1079-7114. DOI: 10.1103/PhysRevLett.75.1226.

[55] Tamás Vicsek and Anna Zafeiris. "Collective motion". en. In: *Physics Reports* 517.3-4 (Aug. 2012), pp. 71–140. ISSN: 03701573. DOI: 10.1016/j.physrep.2012.03.004.

[56] Danelle Devenport et al. "Mitotic internalization of planar cell polarity proteins preserves tissue polarity". en. In: *Nature Cell Biology* 13.8 (Aug. 2011), pp. 893–902. ISSN: 1465-7392, 1476-4679. DOI: 10.1038/ncb2284.

[57] Danelle Devenport. "Tissue morphodynamics: Translating planar polarity cues into polarized cell behaviors". en. In: *Seminars in Cell & Developmental Biology* 55 (July 2016), pp. 99–110. ISSN: 10849521. DOI: 10.1016/j.semcdb.2016.03.012.

[58] Lena P. Basta et al. "Epithelial polarization by the planar cell polarity complex is exclusively non–cell autonomous". en. In: *Science* 387.6740 (Mar. 2025), eads5704. ISSN: 0036-8075, 1095-9203. DOI: 10.1126/science.ads5704.

[59] Mark Zajac, Gerald L. Jones, and James A. Glazier. "Simulating convergent extension by way of anisotropic differential adhesion". In: *Journal of Theoretical Biology* 222.2 (May 2003), pp. 247–259. ISSN: 0022-5193. DOI: 10.1016/S0022-5193(03)00033-X.

[60] Julio M. Belmonte, Maciej H. Swat, and James A. Glazier. "Filopodial-Tension Model of Convergent-Extension of Tissues". en. In: *PLOS Computational Biology* 12.6 (June 2016), e1004952. ISSN: 1553-7358. DOI: 10.1371/journal.pcbi.1004952.

[61] Gaja Lesnicar-Pucko et al. *Cellular mechanisms of chick limb bud morphogenesis*. en. Sept. 2020. DOI: 10.1101/2020.09.10.292359.

[62] Bakhtier Vasiev et al. "Modeling Gastrulation in the Chick Embryo: Formation of the Primitive Streak". en. In: *PLOS ONE* 5.5 (May 2010), e10571. ISSN: 1932-6203. DOI: 10.1371/journal.pone.0010571.